



# Characterization of a new Hencken burner with a transition from a reducing-to-oxidizing environment for fundamental coal studies

Cite as: Rev. Sci. Instrum. **89**, 025109 (2018); <https://doi.org/10.1063/1.5006087>

Submitted: 21 September 2017 . Accepted: 25 January 2018 . Published Online: 14 February 2018

Adewale Adeosun , Qian Huang, Tianxiang Li, Akshay Gopan , Xuebin Wang, Shuiqing Li, and Richard L. Axelbaum



View Online



Export Citation



CrossMark

## ARTICLES YOU MAY BE INTERESTED IN

[Design and characterization of a linear Hencken-type burner](#)

Review of Scientific Instruments **87**, 115114 (2016); <https://doi.org/10.1063/1.4967491>

[A flat flame burner as calibration source for combustion research: Temperatures and species concentrations of premixed H<sub>2</sub>/air flames](#)

Review of Scientific Instruments **65**, 2908 (1994); <https://doi.org/10.1063/1.1144637>

[A small porous-plug burner for studies of combustion chemistry and soot formation](#)

Review of Scientific Instruments **88**, 125106 (2017); <https://doi.org/10.1063/1.5016212>



**MCL**  
MAD CITY LABS INC.

AFM & NSOM      Nanopositioning Systems      Micropositioning      Single Molecule Microscopes

# Characterization of a new Hencken burner with a transition from a reducing-to-oxidizing environment for fundamental coal studies

Adewale Adeosun,<sup>1</sup> Qian Huang,<sup>2</sup> Tianxiang Li,<sup>1</sup> Akshay Gopan,<sup>1</sup> Xuebin Wang,<sup>1,3</sup> Shuiqing Li,<sup>2</sup> and Richard L. Axelbaum<sup>1,a)</sup>

<sup>1</sup>Department of Energy, Environmental and Chemical Engineering, Washington University in St. Louis, St. Louis, Missouri 63130, USA

<sup>2</sup>Department of Thermal Engineering, Tsinghua University, Beijing 100084, China

<sup>3</sup>Department of Thermal Engineering, Xi'an Jiaotong University, Xi'an, Shaanxi 710049, China

(Received 21 September 2017; accepted 25 January 2018; published online 14 February 2018)

In pulverized coal burners, coal particles usually transition from a locally reducing environment to an oxidizing environment. The locally reducing environment in the near-burner region is due to a dense region of coal particles undergoing devolatilization. Following this region, the particles move into an oxidizing environment. This “reducing-to-oxidizing” transition can influence combustion processes such as ignition, particulate formation, and char burnout. To understand these processes at a fundamental level, a system is required that mimics such a transition. Hence, we have developed and characterized a two-stage Hencken burner to evaluate the effect of the reducing-to-oxidizing transition and particle-to-particle interaction (which characterizes dense region of coal particles) on ignition and ultrafine aerosol formation. The two-stage Hencken burner allows coal particles to experience a reducing environment followed by a transition to an oxidizing environment. This work presents the results of the design and characterization of the new two-stage Hencken burner and its new coal feeder. In a unique approach to the operation of the flat-flame of the Hencken burner, the flame configurations are operated as either a normal flame or inverse flame. Gas temperatures and oxygen concentrations for the Hencken burner are measured in reducing-to-oxidizing and oxidizing environments. The results show that stable flames with well-controlled conditions, relatively uniform temperatures, and species concentrations can be achieved in both flame configurations. This new Hencken burner provides an effective system for evaluating the effect of the reducing-to-oxidizing transition and particle-to-particle interaction on early-stage processes of coal combustion such as ignition and ultrafine particle formation. *Published by AIP Publishing.* <https://doi.org/10.1063/1.5006087>

## I. INTRODUCTION

Coal will continue to be important in satisfying the world's primary energy needs due to its global availability and high energy density. Efficient and clean consumption of coal can be achieved through improved technologies that are based on a thorough understanding of fundamental coal combustion processes. The many complex processes associated with coal combustion include particle ignition, volatile release and oxidation, and char burnout. Of special note, the particle ignition time scale plays a critical role in flame stability, char burnout, and formation of particulate matter. Also, flame stability and complete char burnout are important for efficient combustion of coal, but both processes depend on particle ignition. Emission of particulate matter, especially that with aerodynamic diameter below  $2.5 \mu\text{m}$  ( $\text{PM}_{2.5}$ ), is of environmental and health concerns due to the long residence time of such particles in the atmosphere<sup>1–3</sup> and the high toxicity of these particulates if inhaled. Therefore, it is important to understand how various factors, such as the characteristic particle size, coal rank, residence time, particle heating rate, and local combustion condition, affect these various processes

of coal combustion especially coal particle ignition and fine particulate matter formation.

Extensive laboratory studies have provided fundamental insight into single particle ignition.<sup>4–15</sup> Essenhigh *et al.*<sup>4</sup> reviewed fundamental coal ignition studies, and per this review, most ignition studies have focused on the ignition mechanisms, ignition temperatures, and ignition time scales of single coal particles introduced into still and hot gas, usually in an oxidizing condition. Howard and Essenhigh<sup>5</sup> studied single particle ignition and suggested that coal particles can experience homogeneous ignition and heterogeneous ignition simultaneously, depending on the particle size and local combustion conditions. They noted that the ignition mechanism depends on the stoichiometric mixture fraction of the released volatiles in the local combustion environment and on the time scale of particle surface heating relative to the time lag for volatile release. In general, many single particle ignition studies proposed that homogeneous ignition is predominant in a combustion environment with a low heating rate and a large particle size, while the heterogeneous mechanism dominates in a combustion environment with a high heating rate and small particle size.<sup>10,11,13,16</sup> The heating rate is the rate of change of particle temperature with time. However, Wall and other co-authors<sup>7,17</sup> reported that ignition mechanisms and associated temperatures depend more significantly on the

<sup>a)</sup>Author to whom correspondence should be addressed: axelbaum@wustl.edu. Tel.: +1 314-935-7560. Fax: +1 314-935-5464.

surrounding gas condition, local combustion environment, particle heating rate, and injected coal mass for a given coal carrier gas.

Among the various platforms for investigating coal ignition processes, the Hencken burner has gained broad acceptance as its particle heating rate is most representative of a practical pulverized coal boiler.<sup>18–22</sup> The Hencken burner consists of many micro-diffusion flames, and the products of these micro-flames mix rapidly and form a uniform environment due to their short diffusion distances. The uniform environment downstream of these micro-flames can be varied to yield the desired gas temperatures and species concentrations for the injected coal.<sup>22</sup> Because of these features, the Hencken burner has proven to be a valuable platform for fundamental studies of coal particle ignition. These ignition studies not only help in evaluating the effect of gas conditions on the ignition characteristics of particles but also provide improved data for theoretical modeling of ignition. Recent studies have reported the use of the Hencken burner to evaluate the effect of the coal rank and particle heating rates on ignition.<sup>12,13,18–20,23</sup> Kim *et al.*<sup>18</sup> investigated the ignition behavior of coal particles and imaged the ignition process for various coal ranks and particle sizes. The study concluded that high rank coal exhibits homogeneous ignition after primary fragmentation for particle sizes above 150  $\mu\text{m}$ , while low rank sub-bituminous coals ignite homogeneously for particle sizes above 75  $\mu\text{m}$ . Yuan *et al.*<sup>20,23</sup> assessed the ignition behavior for streams of dispersed coal particles at gas temperatures from 1200 to 1800 K. They found a competing interaction between the homogeneous and heterogeneous mechanisms, with the heterogeneous mechanism prevailing at low temperatures for the coal ranks, sizes, and combustion atmosphere studied.

In the near-burner region of a typical pulverized coal (pc) burner, the particle number density is high.<sup>24–29</sup> In this region, the heat from the envelope flame leads to devolatilization in the absence of oxygen such that the coal particles experience a reducing environment. Further downstream, the particles transition from this reducing environment to an oxidizing environment. In this early stage of coal combustion, the particle number density and reducing-to-oxidizing transition are expected to influence the ignition process as well as the evolution of sub-micron particles.<sup>3,30,31</sup> Despite the importance of the reducing zone formed in the near-burner region of pc combustion where coal particle number densities are high, the effects of particle interactions and the reducing-to-oxidizing transition on ignition and aerosol formation have not, to date, been explored.

To this end, a new experimental platform is needed. In this work, a two-stage Hencken burner is described and characterized, wherein particle interactions and the reducing-to-oxidizing transition can be experimentally observed, such that their effect on the ignition process and evolution of sub-micron particles can be evaluated. In this burner, an inner-reducing flame is surrounded by an outer-oxidizing flame. Thus, the two-stage Hencken burner allows coal particles to experience a reducing environment followed by a transition to an oxidizing environment. In a unique approach to the operation of the two-stage Hencken burner, the flame configurations are operated as either normal or inverse flames. The results of the

burner design and characterization for the two-stage Hencken burner and its coal feeder are presented.

## II. EXPERIMENTAL METHODS

### A. Hencken flat-flame burner

The Hencken flat-flame burner is a multi-element non-premixed laminar burner with a heating rate similar to that of conventional pc burners<sup>13,22,23</sup> and wide global “lean” and “rich” flammability limits. This provides for more operational flexibility with respect to the hot gas environment, without the need for cooling the burner.<sup>22</sup> The typical Hencken burner used in coal studies has a central tube for injection of coal that is surrounded by a Hencken burner that yields a specific product temperature and composition. Figure 1 shows a cross section of a two-stage Hencken flat-flame burner. The up-fired burner was designed with a honeycomb structure and a circular cross section to ensure symmetry in the temperature and gas composition. The burner, with an 80-mm diameter, is composed of 570 hypodermic tubes creating an equivalent number of non-premixed flamelets. The hypodermic tubes, all, have an internal diameter of 1.2 mm. The inner flame region consists of 18 non-premixed flamelets. Fuel and oxidizer gases are introduced in separate chambers and are isolated by gasket material. In the “normal” flame configuration, the fuel flows through the tubes and the oxidizer flows through the stainless-steel honeycomb, producing a stream of hot combustion products. We also consider the “inverse” flame configuration, where the flows are reversed, so that the oxidizer flows through the tubes and the fuel through the honeycomb. A central tube with a 2-mm internal diameter (ID) passes through the burner for solid fuel feeding. A quartz tube (150 mm in height) is set above the burner to isolate the burner from the outside environment, decrease heat loss, and provide optical access. A fine stainless-steel wire mesh on top of the quartz tube minimizes disturbances from ambient air and ensures steady convective

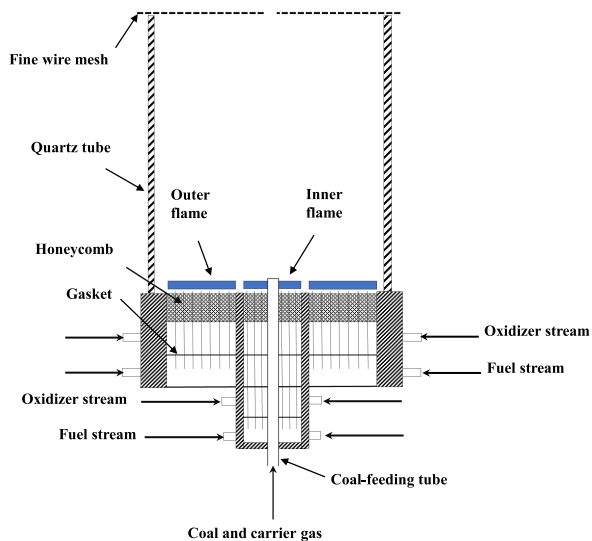


FIG. 1. Cross section of the Hencken flat-flame burner, showing the inner and outer flames.

flow of the post-flame gas. The wire mesh has slots for thermocouple and gas sampling probe insertion into the burner for measurements. The probe is connected to a Horiba PG-250 gas analyzer, which measures the post-flame O<sub>2</sub> concentration based on non-dispersive infrared absorption. The post-flame gas temperatures were measured using a Y-shaped, type-B fine wire thermocouple.

## B. Gas temperature measurement

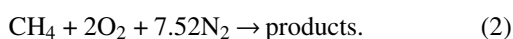
Fine bare wire thermocouples, supported by a ceramic tube, are widely used in measuring high flame temperatures because of their simplicity, cost-effectiveness, good response time, and high spatial resolution.<sup>32–34</sup> A Y-shaped thermocouple configuration was used in this study to simultaneously minimize both radiation and conduction errors from type-B thermocouples. In this design, a two-hole ceramic tube was used to support 200 μm thermocouple bare wires, and 50 μm lead wires were welded to the appropriate ends of the 200 μm thermocouple wires. The 50 μm lead wires were welded together to form a thermocouple with 80 μm bead diameter. The 200 μm thermocouple wires are kept under tension to avoid sagging due to thermal expansion. The resulting thermocouple requires small radiation and conduction corrections. The thermocouple temperatures reported have been corrected for radiation loss following the method of Refs. 32 and 35. See the [supplementary material](#) for the basic theory of radiation and conduction corrections in temperature measurements.

## III. NORMAL AND INVERSE FLAMES, STOICHIOMETRIC MIXTURE FRACTION, AND FLAME STRUCTURE

For this study, the fuel was methane and the oxidizer was a mixture of O<sub>2</sub> and N<sub>2</sub>. The burner was tested under two configurations, both of which had post-flame oxygen concentrations of about 20% on a wet basis. In one configuration, the mixture of O<sub>2</sub> and N<sub>2</sub> is fed through the honeycomb, and the fuel (with or without N<sub>2</sub> dilution) is fed through the tubes. This is referred to as the normal flame configuration. Alternatively, if the oxidizer is introduced through the tubes and the fuel through the honeycomb, this is an inverse flame configuration. The flame structure can be characterized by the stoichiometric mixture fraction,  $Z_{st}$ ,<sup>36–41</sup> given by the following equation:

$$Z_{st} = (1 + Y_{F,0}W_{O,0}v_O/Y_{O,0}W_{F,0}v_F)^{-1}, \quad (1)$$

where  $Y$  denotes the mass fraction,  $W$  is the molecular mass, and  $v$  is the stoichiometric coefficient. The subscripts  $F$ ,  $O$ , and  $0$  refer to the fuel stream, oxidizer stream, and inlet state, respectively. For diffusion flames, the adiabatic temperature is defined for stoichiometric combustion within the limit of the infinite Damkohler number and unity Lewis number. For the methane/air diffusion flame, this stoichiometry is given by the following equation:



If the stoichiometry in Eq. (2) is maintained, nitrogen can be introduced with the fuel only, with the oxidizer only, or split between both the fuel and the oxidizer, all without a change in the adiabatic flame temperature. However, the flame structure, which refers to the relationship between the local temperature and the local gas composition, is altered.<sup>37</sup> Pure CH<sub>4</sub> burning in an O<sub>2</sub>/N<sub>2</sub> mixture corresponds to the lowest  $Z_{st}$ , and CH<sub>4</sub>/N<sub>2</sub> burning in pure O<sub>2</sub> corresponds to the highest. A high  $Z_{st}$  yields more oxygen containing species and less fuel-based species in the high temperature reaction zone. Several studies have demonstrated that increasing  $Z_{st}$  by oxygen enrichment and fuel dilution can inhibit soot formation in diffusion flames, even at high temperatures.<sup>38,40,42</sup> High  $Z_{st}$  can also lead to stronger flames with more resistance to extinction, resulting in a greater extinction scalar dissipation rate and lower extinction temperature.<sup>36</sup> Based on this “flame-design” theory, normal and inverse diffusion flames corresponding to low  $Z_{st}$  and high  $Z_{st}$ , respectively, are considered.

Studies using the Hencken burner for fundamental coal typically report axial profiles of the temperature and oxygen concentration along the centerline of the burner, operated in the low  $Z_{st}$  mode. However, coal particles are dispersed in a jet, expanding out from the coal feed tube. Therefore, a detailed characterization, including radial profiles, is needed to accurately characterize the coal combustion process. Also, radial profile characterization provides information on the axial diffusion length over which the assumption of the radial flatness holds. Thus, we present experimental results that include both axial and radial profiles to identify the degree of uniformity that is attainable in the Hencken burner for normal flames. Gas compositions and temperatures are obtained for both oxidizing and reducing-to-oxidizing atmospheres.

## IV. RESULTS AND DISCUSSION

### A. Flame characterization at low $Z_{st}$

Pulverized coal particles in the near-burner region typically experience combustion environments with local gas temperatures up to 1900 K,<sup>43</sup> and most fundamental studies that use the Hencken burner to study the early stage of coal combustion are conducted up to 1800 K.<sup>18,20,23,44</sup> Table I presents the flow rates in standard conditions with the corresponding superficial exit velocities. Here, three nominal gas temperatures of 1300 K, 1600 K, and 1800 K are achieved by adjusting the flow rates of the fuel and oxidizer gases. The cold superficial flow gas velocities for the inner and outer flames are kept nearly equal to avoid shear-induced radial momentum transfer that can be caused by radial velocity gradients. Three gas temperatures are evaluated at a fixed oxygen concentration of 20%, and all reported oxygen concentration measurements were within 10% standard deviation.

Figures 2(a) and 2(b) show, respectively, the centerline temperature and oxygen concentration measurements for the three temperatures of 1300 K, 1600 K, and 1800 K. The centerline temperatures remain fairly constant above 2 cm height for all temperatures. The lower temperatures below 2 cm are due to the presence of the cold nitrogen carrier gas in the central tube that is used to transport the coal particles. A fixed carrier

TABLE I. Flow rates and gas velocities in oxidizing environment.

Temperature (K)	Flame	Volumetric flow rates (SLPM)				Superficial gas velocity (m/s)
		CH <sub>4</sub>	Fuel N <sub>2</sub>	O <sub>2</sub>	Oxidizer N <sub>2</sub>	
1300	Inner	0.10	...	0.90	1.74	0.24
	Outer	2.86	6.54	23.82	33.33	0.23
1600	Inner	0.27	...	1.13	1.74	0.28
	Outer	3.60	6.54	25.51	31.18	0.23
1800	Inner	0.35	...	1.04	1.64	0.27
	Outer	6.86	15.90	37.71	33.33	0.32

gas flow rate of 130 cm<sup>3</sup>/min is used for all conditions; thus, its influence on centerline gas temperatures decreases near the burner as the gas temperature increases from 1300 K to 1800 K. Figure 2(b) shows that the profiles of the oxygen concentration for the three different temperatures follow similar trends. Thus, with such a relatively constant oxygen concentration profile, the effect of the post-combustion gas temperature on ignition and aerosol formation can be studied using the new two-stage Hencken burner.

Figure 3 presents experimental data to verify the degree of radial uniformity attainable in the Hencken burner for 1300 and 1800 K gas temperatures. Experimental measurements were taken radially over a distance of 30 mm, with the central tube corresponding to the zero position. The gray zone in Fig. 3 corresponds to the inner flame. Radial measurements were taken at several axial positions (1, 3, 6, and 9 cm from the

burner exit). The experimental data indicate that the post-flame combustion environment is symmetric about the central tube. Both gas temperatures and oxygen concentrations become more uniform with a height above the micro-diffusion flames. For measurements at 1 cm above the flame, there are low temperature regions at radial positions between 6 and 10 mm due to heat loss to the central 1-in. ID stainless steel tube that separated the inner flame and the outer flame, as shown in Fig. 1. The low temperature and high oxygen concentration observed for both 1300 K and 1800 K near this central 1-in. ID tube at 1 cm axial position are due to the absence of combustion over the tube and the diffusion of oxygen from the outer flame toward the inner flame. However, above the 1 cm axial position, the profiles are both symmetric radially and uniform axially. Thus, the above results indicate that the two-stage Hencken burner can be used for fundamental studies of coal combustion when the micro-diffusion flames are operated in the normal flame configuration (i.e., at low  $Z_{st}$ ). However, low  $Z_{st}$  flames are prone to soot formation, particularly when using sooty fuels, such as ethylene, as noted in Ref. 45. Soot from the micro-diffusion flames can interfere with the soot formed from coal volatiles during the early stage of coal combustion. Since high  $Z_{st}$  inhibits soot formation,<sup>38,40,42</sup> high  $Z_{st}$  flames can provide a soot-free system for the Hencken burner even at very high temperatures and with sooty fuels.

## B. Flame characterization at high $Z_{st}$

In the normal flame configuration, the mixture of O<sub>2</sub> and most of the N<sub>2</sub> dilution is fed through the honeycomb, and CH<sub>4</sub>, with a little dilution, is fed through the tubes. In other words, the smaller flow rate is fed through the 1.2 mm ID tubes and the larger flow rate through the larger area of the honeycomb. If a high  $Z_{st}$  flame was operated in the normal configuration, the oxygen enrichment and fuel dilution would imply that high gas volume must flow through the 1.2 mm ID tubes, making it difficult to obtain stable flame. To address this concern, the inverse flame configuration is used for the high  $Z_{st}$  flame in the Hencken burner. In the inverse flame configuration, the fuel mixture is fed through the honeycomb, as opposed to the tubes. For high  $Z_{st}$ , the flow rates remain the same as in Table I since the only change is that the nitrogen for dilution is moved from the oxidizer side to fuel side. Figures 4(a) and 4(b) show the centerline temperature and oxygen concentration measurements for the low  $Z_{st}$  and high  $Z_{st}$

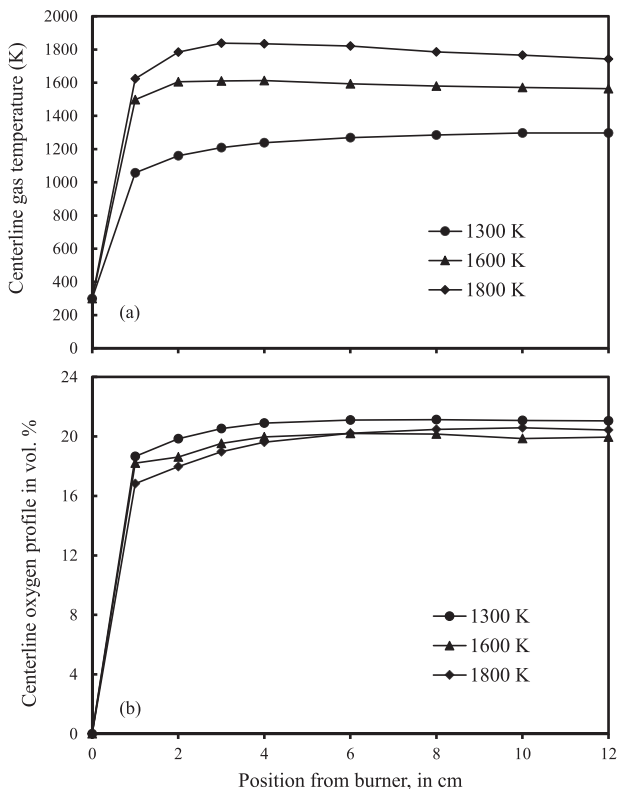


FIG. 2. Measured centerline (a) temperature and (b) oxygen concentration profiles along the height for a normal flame configuration.

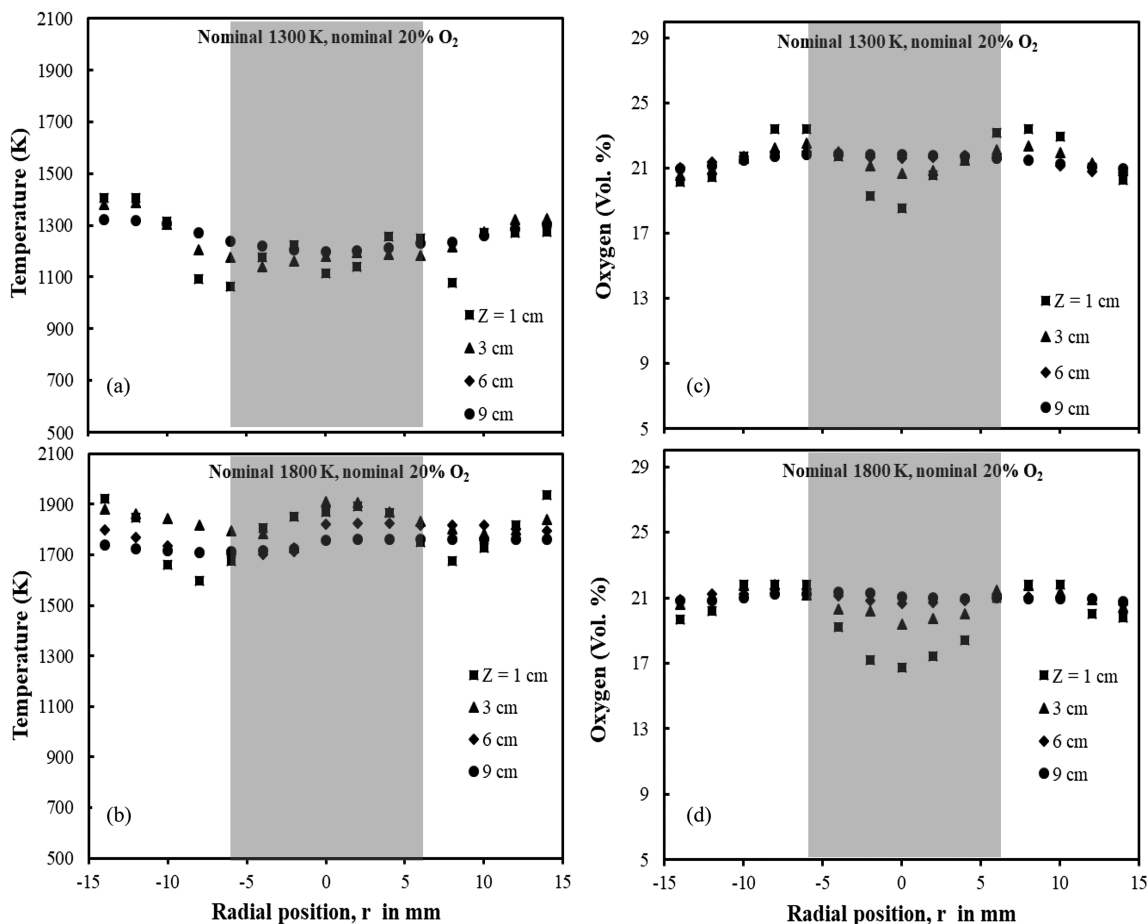


FIG. 3. Measured radial temperature profiles for (a) 1300 K and (b) 1800 K and radial oxygen concentration profiles for (c) 1300 K and (d) 1800 K. The inner flame region is in gray. The particle feeding position is at the zero position.

configurations, respectively. The results for both flame configurations agree well. The lower axial temperatures below 2 cm are due to the cold  $N_2$  carrier gas flow in the central tube for solid fuel transport. The effect of the cold  $N_2$  gas on both the temperature and oxygen concentration profiles dampens out quickly. Since nitrogen gas is used as the carrier gas for the particles at the center, the oxygen concentration at the burner exit is zero. These uniform profiles demonstrate that the new two-stage Hencken burner can be used in both the inverse and normal flame configurations.

Figures 5(a) and 5(b) show flame images taken for inverse and normal flame configurations, respectively. The high  $Z_{st}$ , inverse flame is completely blue, with none of the yellow emissions that is typical for high temperature diffusion flames. Therefore, a high  $Z_{st}$  in the inverse flame configuration would be appropriate for high temperature gas environments and for cases where sooty fuels are used in Hencken burner experiments.

### C. Reducing-oxidizing flame characterization

In a typical pc burner, the coal particles experience reducing environments in regions of high volatile release, despite the oxygen supplied to the coal carrier gas (primary oxidizer). Based on the approach detailed in Ref. 46, a

representative elemental composition of the volatile stream can be obtained from the coal ultimate and proximate analyses presented in Table II. The approach involves subtracting fixed carbon content from the proximate analysis on a dry, ash free basis from the carbon content given in the ultimate analysis also on a dry ash free basis. The quantity obtained is the amount of carbon contained in the volatiles. From this analysis, the C:H:O ratio that characterizes a reducing environment for powder river basin (PRB) coal is approximately 1:3:1, with the oxygen content in the primary oxidizer. In the following study, the inner flame composition was adjusted to give a reducing environment with the desired characteristic C:H:O ratio, so as to mimic a similar reducing condition that is typically created by a dense particle cloud undergoing devolatilization.

For convenience of comparing the effect of a reducing-to-oxidizing (R-O) atmosphere on combustion processes at different temperatures, the centerline height for the transition from the reducing to the oxidizing atmosphere is maintained at 2 cm for all temperatures. Depending on the gas temperature, a height of 2 cm corresponds to an average residence time of 10–20 ms in the two-stage Hencken burner. Since early-stage processes of coal combustion including ignition occurs at these time scales, an average residence time of 10–20 ms was deemed appropriate for characterizing the two-stage Hencken

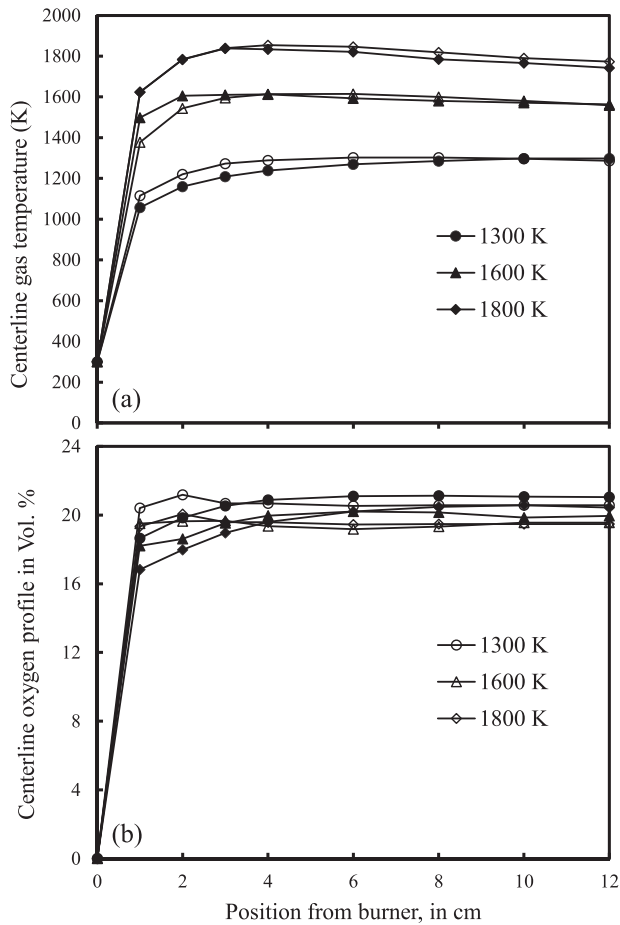


FIG. 4. Comparison of the centerline (a) temperature and (b) oxygen concentration for low  $Z_{st}$  (filled symbols) and high  $Z_{st}$  (open symbols) flame configurations.

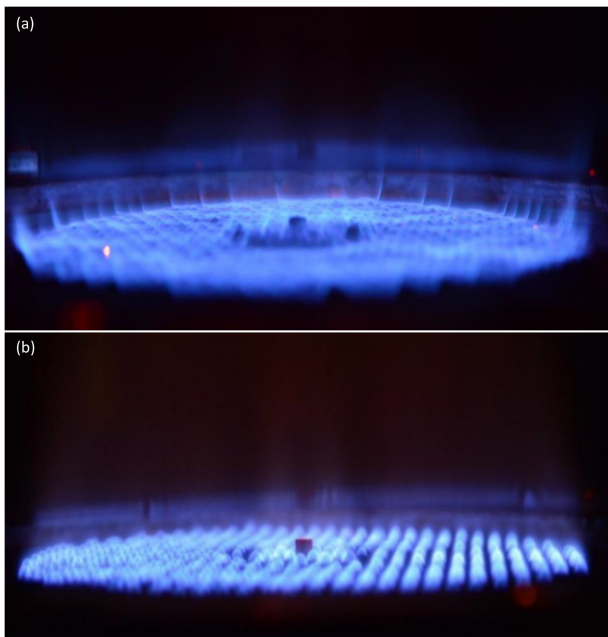


FIG. 5. 1800 K flame images, comparing (a) high  $Z_{st}$  and (b) low  $Z_{st}$  flame configurations.

burner. Table III presents the flow rates in standard conditions for the reducing-to-oxidizing transition flames. Figure 6 presents the centerline temperatures and oxygen mole percent in reducing-to-oxidizing (R-O) transition flames for 1300 K, 1600 K, and 1800 K and further contrasts the results with those of purely oxidizing (P-O) flame environments. The centerline temperature profiles for the R-O transition match extremely well with those of the oxidizing atmospheres for the 1600 K and 1800 K flames.

For the 1300 K gas flame, the temperature is about 200 K lower at 1 cm and about 200 K higher at 2 cm (with 2 cm being the height at which the R-O transition occurs). The observed temperature trend can be explained by mixing. Since the inner flame is rich in fuel for all cases, the fuel molecules need more residence time to mix with oxygen in stoichiometric proportion to burn for the 1300 K case, and the ignition of the inner fuel relies more on heat transfer by conduction from the hot outer post-flame gas products. With the imposed centerline height of 2 cm for the reducing-to-oxidizing transition, the profiles of oxygen downstream of the transition are governed by radial diffusion of  $O_2$  from post-flame gas products of the Hencken burner outer flat-flame. The  $O_2$  concentrations in all cases remain very similar and peak at about 12%–14% on a volume basis. The flame location, seen in Fig. 7, marks the inner reducing flame region at all temperatures.

As the gas temperature increases from 1300 K to 1800 K, the volume and radial spread of the hot gas corona around the flame location increases. This increase is due to the Dufour effect, which is caused by the sharp local concentration gradient between the inner-reducing and outer-oxidizing post-flame gas compositions. The result is hot combustion gases from the outer post-flame diffusing to the flame sheet. Since heat energy is also transferred as species diffuse to the flame location, thus, the corona around the flame location is created by both mass and thermal diffusion due, respectively, to a temperature gradient and a concentration gradient. As the gas temperature increases to 1800 K, the corona widens because more of the products of incomplete combustion break through the flame location and are oxidized in the corona. The radial diffusion of heat and species becomes increasingly significant with temperature. With the results in Figs. 6 and 7, we obtained well-controlled R-O and oxidizing flames at all temperatures. Thus, the new two-stage Hencken burner setup can be used effectively to evaluate the effect of this reducing-to-oxidizing transition on coal ignition and ultrafine particle formation and subsequently compared to oxidizing conditions which are typically studied.

#### D. Coal feeding system

There have been recent efforts to develop new particle feeders with well-dispersed coal particle streams for fundamental coal combustion studies. Yuan *et al.*<sup>23</sup> developed a novel particle feeder based on the principle of deagglomeration. In his design, a programmable piezoelectric ceramic plate vibrates the outlet of a syringe tube containing the coal particles. The high frequency vibration leads to particles impacting the wall of the syringe and then deagglomerating based on

TABLE II. Analysis of PRB sub-bituminous coal.

Proximate analysis (wt. %)				Ultimate analysis (%daf)					
M	VM	FC	Ash	C	H	O	N	S	HHV (MJ/kg)
10	39	42.87	8.14	74.66	5.45	18.24	1.08	0.57	27.45

van der Waals adhesion. Relatively good monodispersion was achieved with a feed rate of  $<70$  mg/min and a variance less than  $\pm 15\%$ . Kim *et al.*<sup>18</sup> used a syringe pump to drive particles into a container at a known rate. A fixed nitrogen flow was then introduced into the container. While these studies achieve well dispersed coal particle streams, they have limited applicability to studies of practical coal combustion processes such as particle cloud ignition. The requirement that the particles must be dried before being fed into the burner further limits the direct interpretation of ignition time scales since moisture vaporization is not accounted for in the particle devolatilization stage.

Similar to the studies of Quann *et al.*<sup>31</sup> and Suriyawong *et al.*,<sup>47</sup> we present a particle feeder that can be used to feed coal particles without drying and to study the effect of particle interactions on coal particle ignition and aerosol formation. Such experimental data are valuable to improve numerical modeling of ignition processes in pc burners. Figure 8 shows a cross section of the coal feeder, which consists of  $\frac{3}{4}$  in. and  $\frac{1}{2}$  in. in ID tubes with the  $\frac{1}{2}$  in. tube driven by a syringe pump. A clear plastic tube containing coal particles is held to the  $\frac{1}{2}$  in. tube by Cajon O-ring fittings. The new coal feeder is uniquely designed with an 8-slot gas distributor, welded slightly above and surrounding the end of a stationary fine gauge 1 mm ID tube. The gas distributor is designed to fit snugly within the plastic tube, creating many high velocity and low momentum jets. These jets emerging from the distributor impact the surface of the coal bed in the plastic tube, entraining the coal particles. The outlet of the fine gauge tube is kept at a constant clearance above the coal particle bed in the plastic tube by matching the coal feed rate to the syringe pump speed.

A pneumatic vibrator attached to an annular plate and installed around the plastic tube locally shakes the surface of the coal bed which keeps the surface loose and enables the high velocity nitrogen gas jet to entrain the coal particles. The rate of entrainment is controlled by the rate at which the plastic tube is driven toward the stationary fine gauge tube.

TABLE III. Flow rates in a reducing-to-oxidizing environment.

Temperature (K)	Flame	Volumetric flow rates (SLPM)			
		CH <sub>4</sub>	Fuel N <sub>2</sub>	O <sub>2</sub>	Oxidizer N <sub>2</sub>
1300	Inner	0.13	...	0.23	1.86
	Outer	2.86	6.54	23.82	33.33
1600	Inner	0.16	...	0.22	1.74
	Outer	3.60	6.54	25.51	31.18
1800	Inner	0.27	...	0.29	1.74
	Outer	6.86	15.90	37.71	33.33

Narrow sized 125-149  $\mu\text{m}$  coal particles are selected for the feeder characterization since this size classification denotes the limit of the particle size range used for fundamental ignition studies<sup>10,48-50</sup> and will be the most difficult to feed based on inertia. For each speed of pump tested and the coal carrier gas flow rate, the experimental run is repeated five times, at

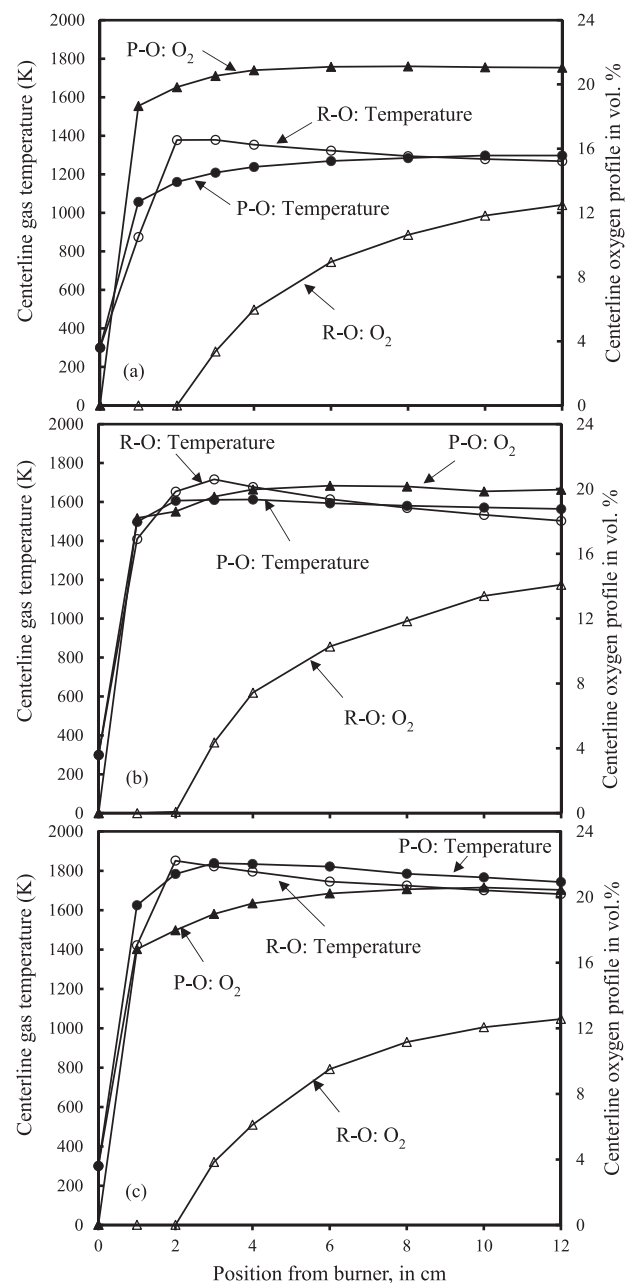


FIG. 6. Comparison of centerline gas temperatures and oxygen concentrations in oxidizing and reducing inner flames for (a) 1300 K, (b) 1600 K, and (c) 1800 K.

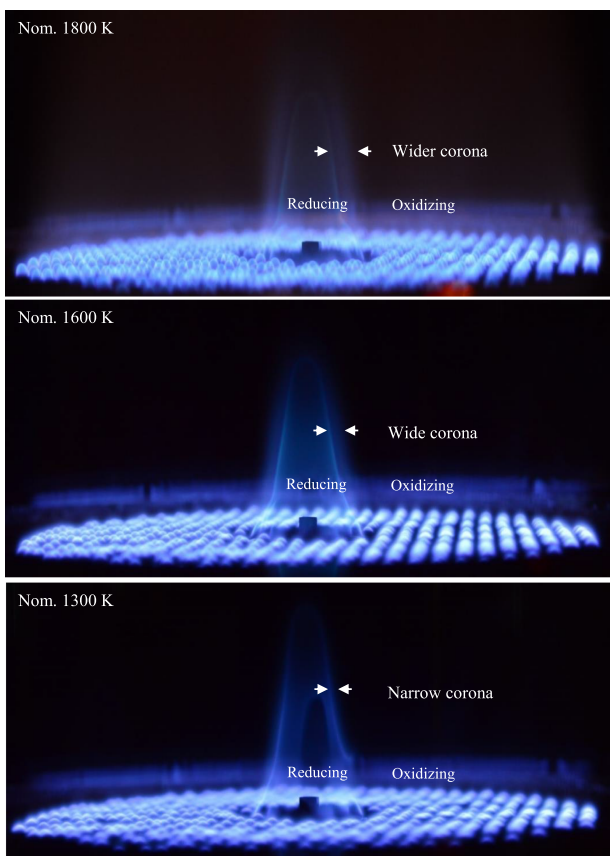


FIG. 7. High resolution images of the reducing-to-oxidizing transition flames.

increments of 3 minutes. The feeder characterization procedure involves weighing the plastic container using a high precision balance before and after each experimental run. The mass of coal fed per unit time can then be determined. To further ensure accurate measurements, the coal fed through the fine gauge tube is collected at the outlet of the burner and compared to the difference in mass in the clear plastic tube before and after each experiment (Fig. 8).

Particle feeding, ranging from single particle feeding to dense particle feeding, can be achieved in the coal feeding system. Figure 9 shows the coal particle feeder characterization for a fixed coal carrier (CC) gas of 130 cm<sup>3</sup>/min of nitrogen and assuming 298 K. This gives a gas velocity higher than the saltation velocity of the coal particles as calculated by the Carman-Kozeny fluidization equation,<sup>51</sup> keeping the particles entrained in the gas. A steady particle feed up to ~500 mg/min can be obtained with a variance of less than ±4%. The particle spacing ratio can be as low as 6 at 298 K, using a gas flow rate of 130 cm<sup>3</sup>/min where the particle spacing ratio is defined as the dimensionless distance between two particles entrained in a carrier gas.

Similar to the approach used by Ref. 23, the particle spacing ratio (PSR) is calculated based on the particle volume fraction, assuming that the particle suspension is mono-disperse with a mean size. Similar to the analysis in Ref. 23, consider a coal feed rate of 33 mg/min, the corresponding standard volumetric rate of the coal can be obtained if the coal density is known (in this case, coal density = 1400 kg/m<sup>3</sup>). The particle

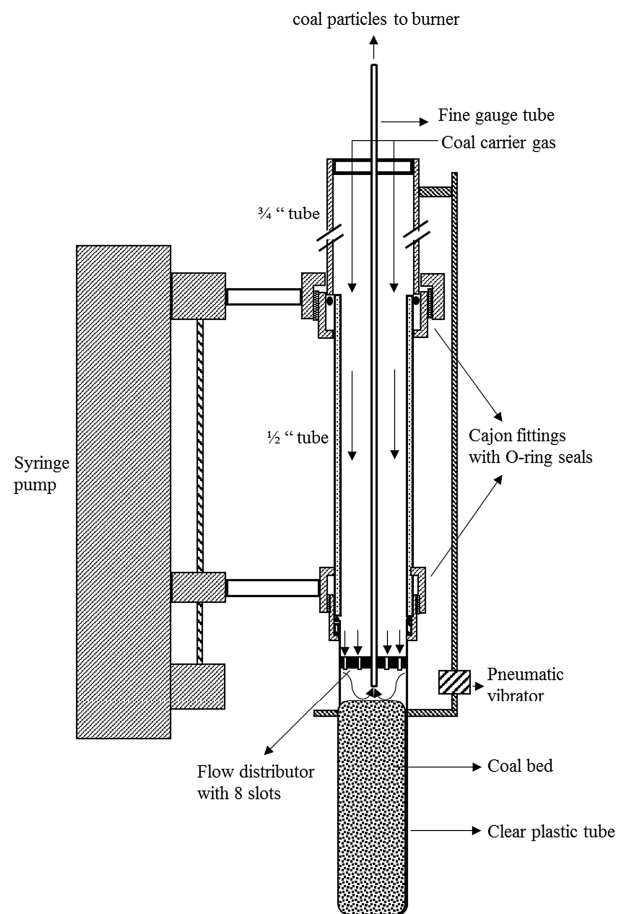


FIG. 8. Cross section of the coal feeder.

volume fraction,  $f_{\text{coal}}$ , can be obtained by dividing the volumetric rate of the coal by the feed flow rate of 0.13 SLPM. Hence, the particle spacing ratio can be obtained by applying a formula of  $\text{PSR} = (\frac{\pi}{6f_{\text{coal}}})^{1/3}$ . The high particle spacing ratio of 14 at 33 mg/min leads to single particle ignition, and the low particle spacing ratio at the feeding rate of 270 mg/min leads to group ignition, as clearly shown in the flame images in Fig. 10. In this work, the coal feeding rate below 100 mg/min is

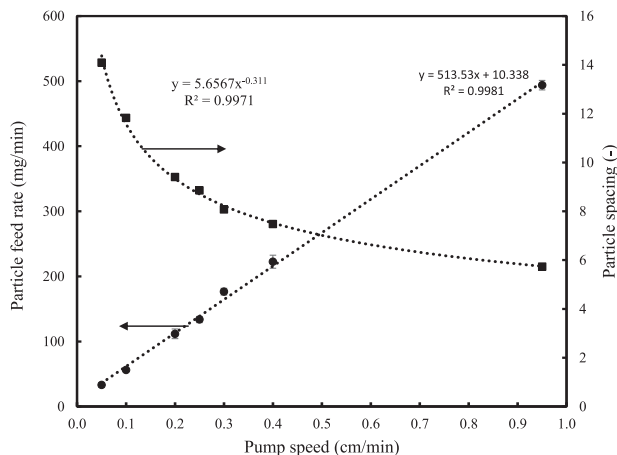


FIG. 9. Coal feeder characterization relating pump speed to the feeding rate and particle spacing.



FIG. 10. High speed camera imaging of coal combustion with different feed rates (a) 33 mg/min and (b) 270 mg/min. The arrow shows the direction of flow of gas and coal particles.

considered to be single particles, consistent with the literature on single particle ignition studies.<sup>18,23,52</sup> Therefore, the coal feeder developed can be used to study single particle ignition as well as group ignition, providing an experimental platform appropriate for evaluating the role of particle interactions and the effect of transition from high to low particle spacing ratios on ignition processes.

The coal particle combustion images are obtained using a NAC MEMRECAM HX-7 high-resolution, high-speed camera at a setting of 2000 frames/s and a shutter speed of 20  $\mu$ s. Figures 10(a) and 10(b) are taken for a coal feed rate of 33 mg/min and 270 mg/min, respectively. Both images are taken at a constant coal carrier gas flow rate of 130 cm<sup>3</sup>/min. Clearly, the particle interactions increase as the particle spacing ratio decreases, and such particle interactions will affect ignition, char burnout, and aerosol formation.

Figure 11 shows the results of changing the coal carrier gas flow rate (CC) for two different syringe pump speeds (PS). For a fixed pump speed, say 0.05 cm/min, doubling the coal carrier gas flow rate from 130 ccm to 304 ccm does not change the coal feed rate. This is expected since increased gas flow does not affect the bed surface position relative to the fine gauge tube but only improves the particle fluidization at the coal bed surface. However, changing the pump speed from 0.05 cm/min to 0.20 cm/min leads to four times the coal feed rate. This increase suggests a linear dependence between the pump speed and particle feed rate, and the increased speed drives more coal particles toward the fine gauge tube through which coal particles are transported to the reaction zone of the two-stage Hencken flat-flame burner.

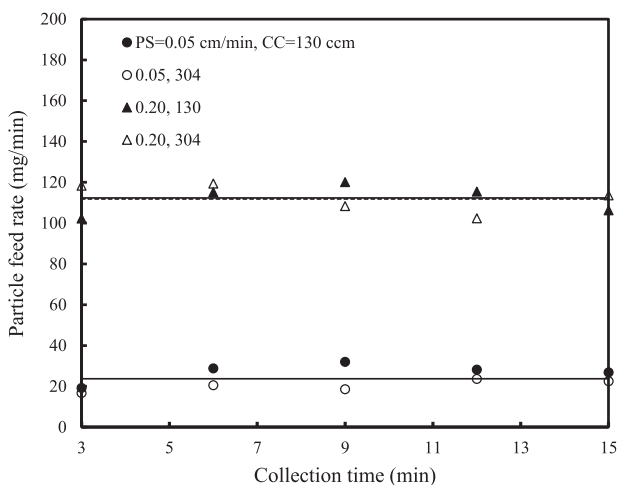


FIG. 11. Effect of the coal carrier gas flow rate on the coal feed rate.

## V. CONCLUSIONS

In practical pulverized coal combustion boilers and furnaces, most coal particles initially go through a reducing environment, characterized by the lack of oxygen in the devolatilization zone, followed by an oxidizing environment. This transition from the reducing to oxidizing environment can affect several of the combustion processes, such as particle ignition, ash formation, and char burnout. However, fundamental laboratory studies typically have either only the oxidizing environment (mimicking the post volatile flame region) or only the reducing environment (mimicking the devolatilization zone) and neglect the effect of this transition from the reducing to oxidizing environment. In this work, a new Hencken burner (flat-flame) design is described, which can mimic the true time-temperature-gas composition history of coal particles in pc boilers. This is achieved by creating a two-stage design, with the inner stage flame operating fuel-rich, with a tunable C:H:O atom ratio characteristic of the volatiles of the coal being studied. The outer stage flame operates fuel-lean with the desired “post-flame” oxygen concentration. Since in practical boilers the devolatilization phase is characterized by a high particle number density, we have also described a new coal feeding system which can be used to study the effects of the particle number density on various processes of coal combustion. Detailed characterization of the burner shows its applicability to various fundamental coal studies.

## SUPPLEMENTARY MATERIAL

See [supplementary material](#) for the basic equation from which key parameters needed for minimizing both conduction and radiation losses are identified.

## ACKNOWLEDGMENTS

This research was funded by the Department of Energy, Award No. DE-FE0009702, and by the Consortium for Clean Coal Utilization at Washington University in St. Louis.

- J. J. Helble and A. F. Sarofim, *J. Colloid Interface Sci.* **128**, 348 (1989).
- M. Neville, R. Quann, B. Haynes, and A. Sarofim, in *Proceedings of Symposium (International) on Combustion* (Elsevier, 1981).
- R. Quann and A. Sarofim, in *Proceedings of Symposium (International) on Combustion* (Elsevier, 1982).
- R. H. Essenhigh, M. K. Misra, and D. W. Shaw, *Combust. Flame* **77**, 3 (1989).
- J. B. Howard and R. H. Essenhigh, *Symp. (Int.) Combust.* **11**, 399 (1967).
- X. Du and K. Annamalai, *Combust. Flame* **97**, 399 (1994).
- T. Wall, R. Gupta, V. Gururajan, and D.-k. Zhang, *Fuel* **70**, 1011 (1991).
- V. S. Gururajan, T. F. Wall, R. P. Gupta, and J. S. Truelove, *Combust. Flame* **81**, 119 (1990).

- <sup>9</sup>C. Zou, L. Cai, D. Wu, Y. Liu, S. Liu, and C. Zheng, *Proc. Combust. Inst.* **35**, 3629 (2015).
- <sup>10</sup>J. Riaza, R. Khatami, Y. A. Levendis, L. Álvarez, M. V. Gil, C. Pevida, F. Rubiera, and J. J. Pis, *Combust. Flame* **161**, 1096 (2014).
- <sup>11</sup>R. Khatami, C. Stivers, and Y. A. Levendis, *Combust. Flame* **159**, 3554 (2012).
- <sup>12</sup>A. Molina and C. R. Shaddix, *Proc. Combust. Inst.* **31**, 1905 (2007).
- <sup>13</sup>C. R. Shaddix and A. Molina, *Proc. Combust. Inst.* **32**, 2091 (2009).
- <sup>14</sup>B. Goshayeshi and J. C. Sutherland, *Combust. Flame* **161**, 1900 (2014).
- <sup>15</sup>B. Goshayeshi, "Coal combustion simulation using one-dimensional turbulence model." Ph.D. dissertation (The University of Utah, 2014).
- <sup>16</sup>T. Maffei, R. Khatami, S. Pierucci, T. Faravelli, E. Ranzi, and Y. A. Levendis, *Combust. Flame* **160**, 2559 (2013).
- <sup>17</sup>D. Zhang and T. F. Wall, *Fuel* **73**, 647 (1994).
- <sup>18</sup>R.-G. Kim, D. Li, and C.-H. Jeon, *Exp. Therm. Fluid Sci.* **54**, 212 (2014).
- <sup>19</sup>Y. Liu, M. Geier, A. Molina, and C. R. Shaddix, *Int. J. Greenhouse Gas Control* **5**(Supplement 1), S36 (2011).
- <sup>20</sup>Y. Yuan, S. Li, F. Zhao, Q. Yao, and M. B. Long, *Fuel* **184**, 1000 (2015).
- <sup>21</sup>Z. Xiao, T. Shang, J. Zhuo, and Q. Yao, *Fuel* **181**, 1257 (2016).
- <sup>22</sup>S. Li, Y. Ren, P. Biswas, and S. D. Tse, *Prog. Energy Combust. Sci.* **55**, 1 (2016).
- <sup>23</sup>Y. Yuan, S. Li, G. Li, N. Wu, and Q. Yao, *Combust. Flame* **161**, 2458 (2014).
- <sup>24</sup>K. Annamalai and P. Durbetaki, *Combust. Flame* **29**, 193 (1977).
- <sup>25</sup>K. Annamalai and W. Ryan, *Prog. Energy Combust. Sci.* **18**, 221 (1992).
- <sup>26</sup>K. Annamalai, W. Ryan, and S. Dhanapalan, *Prog. Energy Combust. Sci.* **20**, 487 (1994).
- <sup>27</sup>X. Du, C. Gopalakrishnan, and K. Annamalai, *Fuel* **74**, 487 (1995).
- <sup>28</sup>W. Ryan and K. Annamalai, *J. Heat Transfer* **113**, 677 (1991).
- <sup>29</sup>W. Ryan, K. Annamalai, and J. Caton, *Combust. Flame* **80**, 313 (1990).
- <sup>30</sup>M. Neville and A. F. Sarofim, *Symp. (Int.) Combust.* **19**, 1441 (1982).
- <sup>31</sup>R. J. Quann, M. Neville, M. Janghorbani, C. A. Mims, and A. F. Sarofim, *Environ. Sci. Technol.* **16**, 776 (1982).
- <sup>32</sup>V. Hindasageri, R. Vedula, and S. Prabhu, *Rev. Sci. Instrum.* **84**, 024902 (2013).
- <sup>33</sup>D. Bradley and K. Matthews, *J. Mech. Eng. Sci.* **10**, 299 (1968).
- <sup>34</sup>D. De, *J. Inst. Energy* **54**, 113 (1981).
- <sup>35</sup>M. V. Heitor and A. L. N. Moreira, *Prog. Energy Combust. Sci.* **19**, 259 (1993).
- <sup>36</sup>R. Chen and R. Axelbaum, *Combust. Flame* **142**, 62 (2005).
- <sup>37</sup>D. X. Du, R. L. Axelbaum, and C. K. Law, *Symp. (Int.) Combust.* **23**, 1501 (1991).
- <sup>38</sup>B. Kumfer, S. A. Skeen, and R. L. Axelbaum, *Combust. Flame* **154**, 546 (2008).
- <sup>39</sup>B. Kumfer, S. Skeen, R. Chen, and R. Axelbaum, *Combust. Flame* **147**, 233 (2006).
- <sup>40</sup>S. Skeen, G. Yablonsky, and R. Axelbaum, *Combust. Flame* **157**, 1745 (2010).
- <sup>41</sup>F. Xia, G. S. Yablonsky, and R. L. Axelbaum, *Proc. Combust. Inst.* **34**, 1085 (2013).
- <sup>42</sup>S. Skeen, G. Yablonsky, and R. Axelbaum, *Combust. Flame* **156**, 2145 (2009).
- <sup>43</sup>Z. Huque, M. R. Ali, and R. Kommalapati, *Fuel Process. Technol.* **90**, 558 (2009).
- <sup>44</sup>Y. Yuan, S. Li, and Q. Yao, *Proc. Combust. Inst.* **35**, 2339 (2015).
- <sup>45</sup>Q. Gao, S. Li, Y. Yuan, Y. Zhao, and Q. Yao, *Energy Fuels* **30**, 1815 (2016).
- <sup>46</sup>I. ANSYS, Release 12.0, 2009.
- <sup>47</sup>A. Suriyawong, M. Gamble, M.-H. Lee, R. Axelbaum, and P. Biswas, *Energy Fuels* **20**, 2357 (2006).
- <sup>48</sup>R. Khatami and Y. A. Levendis, *Combust. Flame* **164**, 22 (2016).
- <sup>49</sup>I. Smith, in *Proceedings of Symposium (International) on Combustion* (Elsevier, 1982).
- <sup>50</sup>H. Zhang and J. Zhang, *Combust. Flame* **153**, 334 (2008).
- <sup>51</sup>J. Coulson, J. Richardson, J. Backhurst, and J. Harker, *Particle Technology and Separation Processes* (Butterworth-Heinemann, Oxford, 1991), Vol. 2.
- <sup>52</sup>H. Lee and S. Choi, *Combust. Flame* **162**, 2610 (2015).